Nonexponential relaxations in dense microemulsion near the glasslike transition

Eric Y. Sheu
Exxon Research & Engineering Company, Annandale, New Jersey 08801

Sow-Hsin Chen
Department of Nuclear Engineering and Center for Material Science and Engineering, Massachusetts Institute of Technology, Cambridge, Massachusetts 02139

J. S. Huang and J. C. Sung
Exxon Research & Engineering Company, Annandale, New Jersey 08801

(Received 19 October 1988; revised manuscript received 16 January 1989)

Extensive quasielastic-light-scattering, small-angle neutron scattering, and neutron-spin-echo (NSE) spectroscopic measurements have been performed on a three-component microemulsion system containing bis(2-ethylhexylsulfosuccinate) (AOT) (surfactant), D_2O, and decane (oil) at two temperatures in the one-phase region. By fixing the molar ratio of water to AOT at $w=40.61$, the average radius of spherical surfactant coated water droplets can be maintained at 58 Å with a polydispersity index of 22%. The volume fraction ϕ of the droplets can be continuously varied from 0.1 to 0.75, spanning the entire range from the dilute gas all the way to the close-packed glass by adjusting the oil content of the microemulsion. The static structure factors and the time-dependent density correlation functions of these densely packed spherical droplets were systematically measured as a function of the volume fraction. As ϕ increases from 0.1 to 0.75, the structure factor gradually evolves from a smooth function of the order unity into a highly oscillatory function, with the height of the first diffraction peak around 2 and higher, similar to that of a dense liquid. At the same time the time-dependent density correlation function exhibits pronounced nonexponential relaxation. The Kohlrausch-Williams-Watts (KWW) stretched exponential function, $\exp[-(t/T)^{\beta}]$, has been shown to fit the density correlation function over most of the time range of the measurements, which covers nearly three decades, at Q values of about 10^{-3} Å^{-1}, typical in a light scattering experiment. The exponent β, starting from an initial value of unity at $\phi=0.1$, gradually decreases to about 0.6 at $\phi_c \sim 0.65$ and increases thereafter. The relaxation time T shows a trend to diverge at $\phi \sim \phi_c$, approximately following the Vogel-Fulcher law. These features bear striking similarity to a glasslike transition predicted by recent mode-mode coupling theories of dense liquids. The KWW function also fits very well the time-dependent density correlation function at $\phi=0.6$, measured by NSE ($Q \sim 0.2$ Å^{-1}). Thus, the KWW function is shown to be valid for the Q range spanning from 0.001 to 0.2 Å^{-1}. The relaxation time, to a good approximation, scales like $Q^{-2/\beta}$.

I. INTRODUCTION

In general, a microemulsion is a thermodynamically stable five-component mixture of water (with a small amount of salts added), oil, surfactant, and cosurfactant (short-chain alcohol). For certain compositions of these five components, a single-phase, isotropic and optically clear liquid solution can be obtained which contains colloidal particles of size of the order of 100 Å. Water/decane/AOT (anionic surfactant), in particular, is a model microemulsion in the sense that it is a three-component system and the single-phase microemulsion is obtainable in a substantial portion of its ternary phase diagram at room temperature.[1]

Previous light scattering and neutron scattering experiments[2,3] have established that near the oil corner of the ternary phase diagram, an AOT/water/decane microemulsion consists of surfactant-coated spherical water droplets dispersed in an oil continuous medium. The size of the water core of the droplet is a function of a parameter w which is the molar ratio of water to surfactant, i.e., the number of water molecules per surfactant molecule in the solution. Kotlarchyk, Chen, and Huang have shown that these droplets are polydispersive, having a polydispersity index $p \sim 0.3$. The average radius $\bar{R}$ of the droplet can be accurately calculated by a formula[4,5]

$$(1+2p^2)\bar{R} = \frac{3v_w}{a_H} w + \frac{3v_H}{a_H} , \tag{1}$$

where v_w is the volume of a water molecule, v_H is the volume of the head group of an AOT molecule, and a_H is the head area per AOT molecule in the droplet. In practice, $\bar{R}$ is a function of temperature because the parame-

ters a_H and p are temperature dependent. However, the dependence of $\bar{R}$ and p on the volume fraction of the droplet is expected to be weak.[5] It has also been shown by Kotlarchyk, Chen, Huang, and Kim[6] that near the center of the phase triangle, where the volume fraction of oil and water are equal and the surfactant volume fraction is appreciable, the microemulsion can be regarded as a system of densely packed spheres of an average radius $\bar{R}+\Delta$, Δ being the length of the surfactant molecule. Further evidence of the droplet structure in AOT/H_2O/decane microemulsion was provided by observations of phase separation and critical phenomena in a system where the value w was chosen to be 40.61.[7,8] Under this condition the radius of the water core of the microemulsion droplets has a constant value of 50 Å and one can vary the volume fraction of the droplets ϕ by varying the volume fraction of oil according to a relation $\phi=1-\phi_{\text{oil}}$. Figure 1 is a phase diagram for microemulsions made with $w=40.61$. This condition can in practice be realized by taking the AOT to water ratio as 3 gm of AOT per 5 ml of water, and a variable amount of oil. Hence we call these microemulsions 3/5 systems. For volume fractions between 0.03 and 0.40, if one heats up the microemulsions, they will phase separate at certain temperatures called cloud points. Below the cloud points a microemulsion is in a single phase. Above the cloud points the microemulsion separates into two microemulsion phases containing different volume fractions of the droplets.[5] The cloud point curve, in this sense, can be neglected as a coexistent curve of a pseudobinary system consisting of the droplets and oil. At temperatures around 40 °C, if one increases the volume fraction of the droplets above 60%, the single-phase microemulsion will undergo a first-order phase transition to a lamellar phase where the droplets no longer exist. The single-phase microemulsion we are interested in in this paper is normally denoted as L_2 phase.[9] For temperatures below 30 °C and above 15 °C the L_2 microemulsions can be well represented as collections of surfactant-coated water sphers of an average radius 50 Å dispersed in oil continuous media. The volume fraction of these droplets can be varied continuously from 0.03 to 0.75 without being interrupted by the lamellar phase.

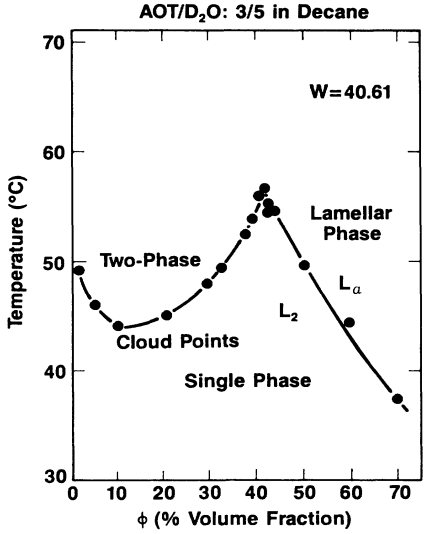

FIG. 1. Boundaries between the one-phase microemulsions, denoted by L_2, and the two-phase microemulsions, called a cloud point curve (coexistence curve), and between that and the lamellar liquid-crystalline phase, denoted by L_α, for a system of three-component microemulsion, AOT/D_2O/decane, at a constant water to AOT molar ratio, $w=40.61$. The ordinate is the temperature and the abscissa is the volume fraction of water plus AOT (Refs. 9 and 29). Experimental paths used in this paper correspond to horizontal lines with temperatures equal to 17.9 °C and 22.6 °C.

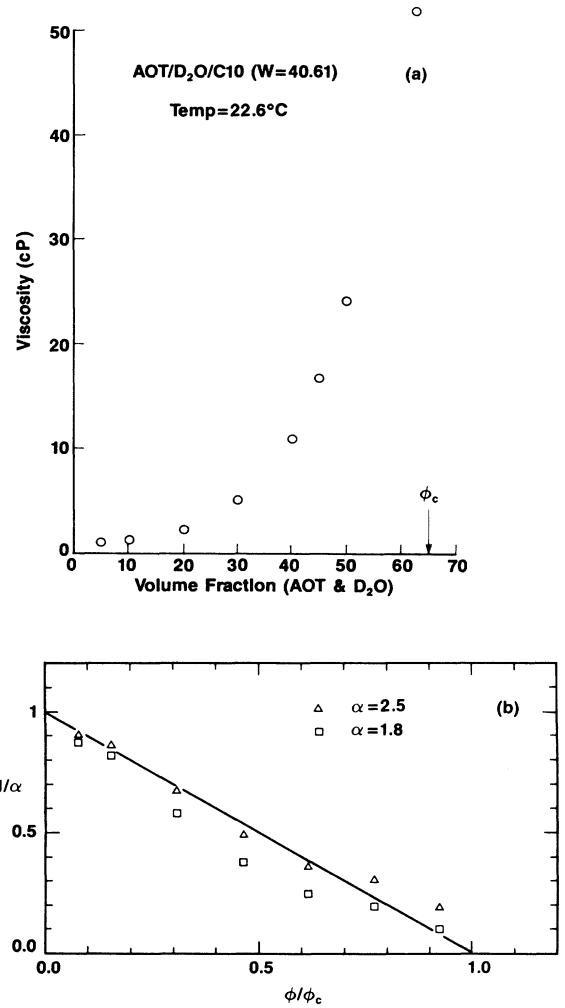

FIG. 2. Shear viscosity η of $w=40.61$ microemulsions as a function of volume fraction $\phi=\phi_{\text{AOT}}+\phi_{D_2O}$ at a temperature 22.6 °C. 2(a) is the actual data and 2(b) is a reduced plot of $(\eta_s/\eta)^{1/\alpha}$ vs (ϕ/ϕ_c), where η_s is the shear viscosity of decane and $\phi_c=0.65$ is the critical volume fraction defined in the text. Squares represent the data reduced by $\alpha=1.8$ and triangle by $\alpha=2.5$. The solid line is the theoretical prediction described in Sec. IV (Ref. 29).

In this paper we shall exploit the fact that the L_2 microemulsions can be regarded as dense liquids with continuously variable particle packing fractions. We are thus able to investigate the dynamics of density fluctuation of these droplets by dynamic light scattering and neutron-spin-echo spectroscopy. An exciting possibility is to be able to test the recently developed mode-mode coupling theory of the dynamics of dense fluids.[10,11] Especially, we would like to observe dynamic singularities of glasslike transitions predicted by these theories.[10–16] Our starting observation is that the shear viscosity of the microemulsions at a temperature of 22.6 °C increases rapidly as a function of volume fraction ϕ of the droplets and is seemingly divergent at a critical volume fraction $\phi_c = 0.65$ as shown in Fig. 2(a). In the following sections we shall describe the experiments which were designed to look at both static and dynamic properties of the microemulsion near ϕ_c in detail.

II. EXPERIMENTS

A. Samples

Bis(2-ethylhexylsulfosuccinate) (AOT) used in this experiment was from Fluka Chemical Company. AOT was purified by first dissolving it in methanol to precipitate out salt impurities. The solution was then filtered and methanol evaporated by rotating vacuum method at 30 ° C. We then redissolve the residues obtained from the previous step in hexane, containing activated charcoal, to remove the unsulfonated maleic ester, and finally filter the solution and evaporate the haxane at room temperature. D_2O used was gold label with a deuterium atom constant of greater than 99.8%. Decane was also of gold label, both from Aldrich Chemical Company.

The AOT/D_2O/decane microemulsion was prepared first by making an AOT reversed micelle solution in decane followed by an addition of the proper amount of D_2O. The molecular ratio of water to AOT, denoted as w, for all the microemulsion systems studied, was chosen to be 40.61, which is equivalent to 3 g of AOT in 5 ml of D_2O. The volume fraction ϕ represents the total volume fractions of AOT plus D_2O with AOT molecular volume taken to be 612 Å^3.[5,17]

B. Quasielastic light scattering

A He/Ne laser of wavelength 6328 Å and 15 mW power together with a Brookhaven Instrument model Bi-2030AT 128-channel digital correlator were used to perform light scattering measurements. The magnitude of the scattering vector $|\mathbf{Q}|$ was tuned by changing the scattering angle in a range from 30° to 130°. The measurements were performed at seven different scattering angles, spanning a Q range from 1.4×10^{-3} Å^{-1} to 2.54×10^{-3} Å^{-1}. Toluene was used as an index matching fluid to reduce background scattering from the cylindrical quartz cell. Temperature of the sample was controlled by a NESLAB water circulating temperature bath having ±0.1 °C control accuracy.

In order to pickup both fast and slow relaxations of the time-dependent density correlation function, multiple sampling time mode of the correlator was used in the process of data collection. The duration of each run was selected such that the time-dependent density correlation function $C(t)$ reaches a statistical error of 0.1% or less for every time channel, i.e., the counts of each channel are at least 1.0×10^6 after subtracting the background counts.

C. Small-angle neutron scattering

SANS experiments were performed at 9HB beam line of High Flux Beam Reactor at Brookhaven National Laboratory. The neutron wavelength was selected to be 4.5 Å by a multilayer monochrometer. The neutron flux at this wavelength was 1.1×10^6 neutrons/cm^2/s with $\Delta\lambda/\lambda = 0.08$. A two-dimensional area detector of 50×50 cm^2 with 128×128 pixels was used to detect the scattered neutrons. The sample-to-detector distance was chosen to be such that Q ranges from 0.01 to 0.3 Å^{-1}. $Q=(4\pi/\lambda)\sin(\theta/2)$ is the magnitude of Bragg wave vector and θ is the scattering angle. The data reduction follows a procedure published previously.[18]

D. Neutron-spin-echo spectroscopy

Measurements of the time-dependent density correlation function of the AOT microemulsion system at high-Q values ($Q=0.086$ to 0.185 Å^{-1}) were carried out at IN11 neutron-spin-echo spectrometer at the Institut Laue–Langevin in Grenoble, France.[19] The energy transfer of neutrons in the quasielastic scattering process was obtained directly through measurements of the Larmour precessions of the individual neutron spin in an external magnetic field. The collected intensity was then reduced by a standard procedure to subtract out the contribution from incoherent scattering.[20] By this data reduction, the normalized intermediate scattering function, $I(Q,t)/S(Q)$, can be obtained in this type of measurement, which is equivalent to the time-dependent density correlation function measured by the dynamic light scattering. Measurements at four different Q values, 0.086, 0.111, 0.136, and 0.185 Å^{-1}, were performed for a $\phi=0.6$ sample at 22.6 °C.

III. RESULTS

We shall present the results of SANS, QELS, and NSE measurements in Secs. III A–III C, respectively.

A. Small-angle neutron scattering

For a system of polydisperse spheres, having a Schultz distribution in size,[1] the intensity distribution of small-angle neutron scattering can be expressed concisely as

$$I(Q)=(\Delta\rho)^2\phi_w\left[\frac{4\pi}{3}\bar{R}^3\right]\frac{(z+6)(z+5)(z+4)}{(z+1)^3}\times\langle\tilde{P}(Q)\rangle\langle S(Q)\rangle\ , \tag{2}$$

where $\Delta\rho$ is the contrast between D_2O and the hydrocar-

bon in the solvent, ϕ_w the volume fraction of water, $\bar{R}$ the mean radius of the water core in the microemulsion droplet, z the width parameter in the Schultz distribution,[21] and the size-averaged particle structure factor is defined as

$$\langle \tilde{P}(Q) \rangle = \langle R^6 \tilde{P}(Q,R) \rangle / \langle R^6 \rangle \ . \quad (3)$$

$\tilde{P}(Q,R)$ in this expression being the normalized particle structure factor of a sphere of radius R $[3j_1(QR)/QR]^2$, where $j_1(x)$ is the spherical Bessel function of the first-order. $\langle S(Q) \rangle$ is the size-averaged interdroplet structure factor[22] which is the Fourier transform of the effective pair correlation function of the droplet.

Since information on the interparticle interactions between droplets are not precise at the present time, $\langle S(Q) \rangle$ could not be computed reliably by a statistical mechanical theory. We took a point of view of extracting experimentally $\langle S(Q) \rangle$ using a knowledge of the parameters from a previous analysis of $\langle \tilde{P}(Q) \rangle$.[5] We chose $\bar{R} = 50$ Å and $z = 20$ as Schultz distribution parameters to compute $\langle \tilde{P}(Q) \rangle$ according to Eq. (3). Then, $\langle S(Q) \rangle$ was obtained by dividing $I(Q)$ by the known prefactor and $\langle \tilde{P}(Q) \rangle$. Figure 3 shows the average structure factors thus extracted for $\phi = 0.75$, 0.65, and 0.55. Three features of these curves should be noted: (a) the values of $\langle S(Q=0) \rangle$ are very low, indicating a strong repulsive interaction resulting in low osmotic compressibilities, (b) the first diffraction peaks of height ~ 2.0 occuring at $Q_1 \sim 0.079$ Å^{-1}, (c) the second diffraction peaks of height ~ 1.2 occuring at $Q_2 \sim 0.14$ Å^{-1}. It should also be remarked that these size-averaged structure factors generally have the first diffraction peak heights lower than the corresponding structure factors of the monodisperse systems but their peak positions are nearly the same.[23] It is therefore of interest to infer the average interparticle distance D, from Q_1 according to an empirical formula known to be valid in describing correlation peaks in dense micellar systems,[24,25]

$$Q_1 D = 6.8559 + 0.0094 D \ . \quad (4)$$

From this equation, using $Q_1 = 0.079$ Å^{-1}, we get $D = 99$ Å which is about twice the $\bar{R} = 50$ Å used to extract these curves. Since the microemulsion droplets are water droplets coated with $a \sim 8$ Å surfactant layer, this estimate indicates that at such high volume fractions, the surfactant layers probably overlap and the droplet systems are percolated. This seems to be supported by an independent experiment on electric conductivity for such systems performed by Kim and Huang.[26]

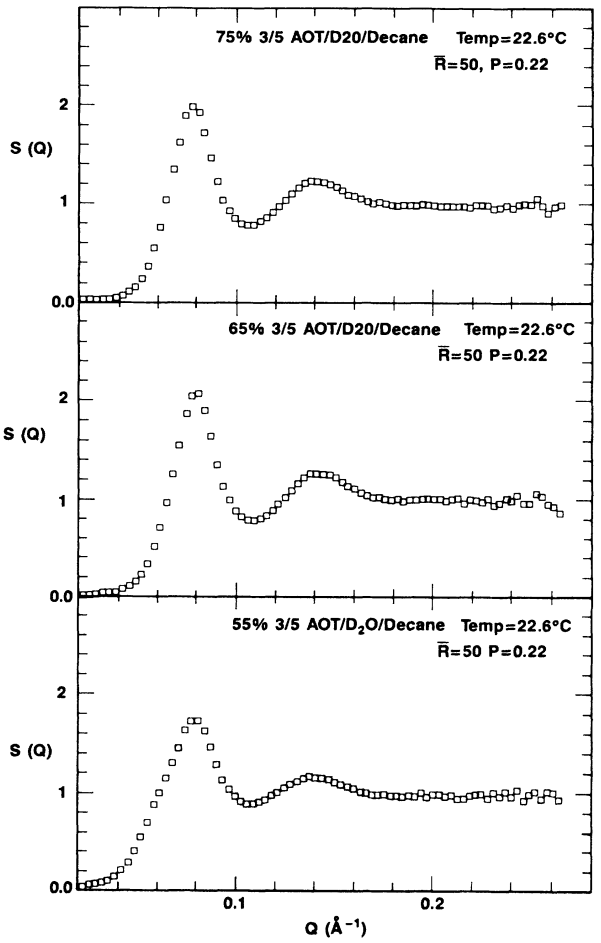

FIG. 3. Interdroplet structure factors extracted from SANS data at $\phi = 0.75$, 0.65, and 0.55 assuming an average droplet size $\bar{R} = 50$ Å and polydispersity index of 0.22, taken from a previous analysis (Ref. 5). A notable feature is the sharp first diffraction peak having height in the vicinity of 2.0 followed by a second diffraction peak occurring at approximately twice the Q_{max} value of the first. This feature is characteristic of a dense liquidlike structure.

B. Quasielastic light scattering

The photon correlation function measured in this experiment is the time-dependent density correlation function $\langle \rho_Q(0) \rho_Q(t) \rangle / \langle \rho_Q^2 \rangle$, denoted by $C(t)$ which is normalized such that $C(0) = 1$. The sampling time used was 2.5 μs and a multiple sampling time mode was used to measure the correlation function up to 1400 μs. Some typical examples of the photon correlation function are displayed in Fig. 4. Figure 4(a) shows $\ln[C(t)] + 5$ versus t (ms) for three volume fractions, 0.1, 0.5, and 0.65 at a temperature of 22.6 °C. It is easily seen that, while for $\phi = 0.1$ the decay is exponential, the decay is clearly nonexponential showing considerable long time tails for $\phi = 0.5$ and 0.65. Figure 4(b) displays the $C(t)$ at three volume fractions, 0.2, 0.5, and 0.68, for the low-temperature case (temperature 17.9 °C). A striking feature, which is not seen in Fig. 4(a), should be noted. While for $\phi = 0.2$, $C(t)$ decays to zero at long time, for the other two higher volume fraction cases, $C(t)$ seem to decay to a nonzero constant (DC) at long time. It is worth noting that the measured background starts to deviate from the calculated ones ($\sim 10\%$ higher) as $\phi \geq 0.60$. We are attempting to determine this DC component more accurately in the future. But in this paper

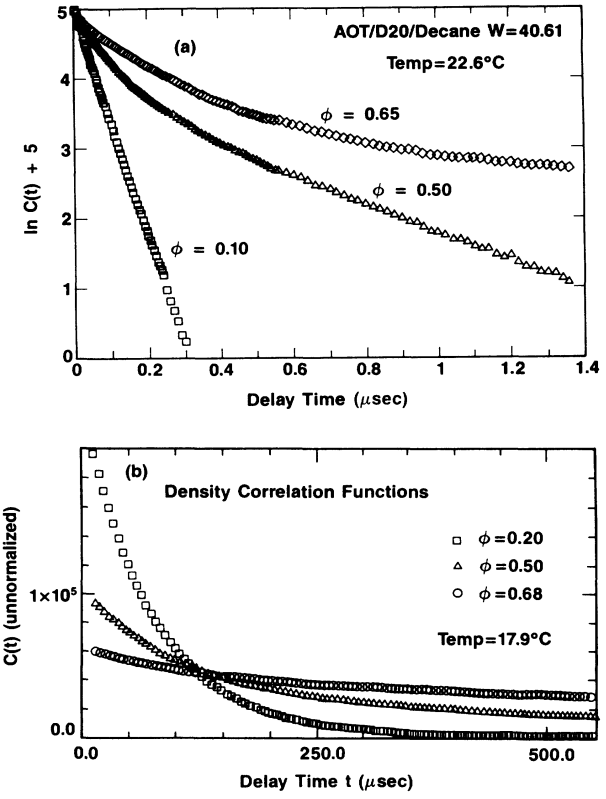

FIG. 4. (a) Normalized time-dependent density correlation function for $w=40.61$ AOT/D_2O/decane microemulsions at $\phi=0.65$, 0.50, and 0.10 and at a temperature of 22.6 °C. The ordinate is in a logarithmic scale and the abscissa is in linear time scale of millisecond. Note the increasingly pronounced deviation from exponential behavior as ϕ increases. (b) Unnormalized time-dependent density correlation functions for $\phi=0.68$, 0.5, and 0.2 at a temperture of 17.9 °C. The feature to be noted is the sharp decrease of the amplitude of the initial decay of the correlation functions as ϕ increases. This is accompanied by development of long time tails which seem to contain a DC part.

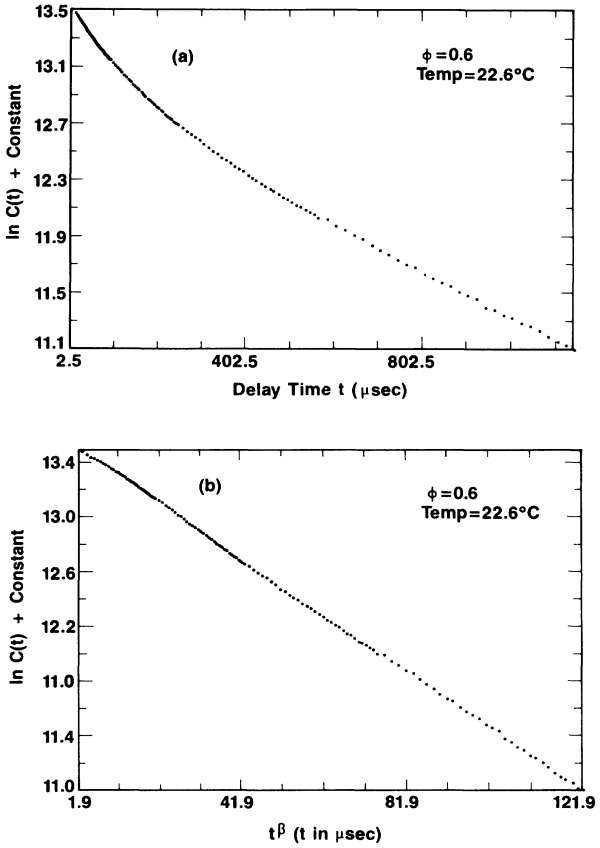

FIG. 5. Stretched exponential behavior of a time-dependent density correlation function $C(t)$. (a) Logarithm of $C(t)$ vs t plot for t from 2.5 μs to 1140 μs. (b) The same $\ln[C(t)]$ plotted as a function of t^{β} with $\beta=0.68$ This figure illustrates vividly that the stretched exponential behavior is valid for decay time longer than 100 μs.

we uniformly subtracted the measured background, which is taken from the delayed channels (1000 channels delayed), prior to data fitting. After the background subtractions, these curves can all be fitted to a Kohlrausch-Williams-Watts (KWW) function of the following form:

$$C(t)=\exp[-(t/\tau)^{\beta}] \ . \tag{5}$$

Figure 5 illustrates the applicability of Eq. (5) vividly. In Fig. 5(a) we display $\ln[C(t)]$ versus t (μs) in a linear scale. The curve, spanning delay time between 2.5 and 1200 μs, is clearly not a straight line. However, in Fig. 5(b), the same curve, when displayed in terms of a coordinate of a stretched time t^{β}, where $\beta=0.68$, shows a good straight line for the delay time in the range of $100<t<1200$ μs. The slope of this curve is just $T^{-\beta}$.

It is perhaps of interest at this point to digress a bit and discuss whether the above-mentioned stretched exponential function can be produced as a result of polydispersity or by some other known mechanism of particle aggregation. Figure 6 shows a computer-simulated result of $C(t)$ for a collection of independent Brownian particles of an average radius 65 Å, having a Schultz size distribution. The solid curve corresponds to a case with a polydispersity index, $p=0.3$ while the dotted curve corresponds to the monodisperse case. It is obvious that the effect of polydispersity on $C(t)$ is to produce a slightly longer decay time but this effect alone is not enough to simulate the stretched exponential function with a β appreciably less than unity. Figure 7 illustrates this latter point more precisely. One other possibility for producing a long time tail for $C(t)$ is via a particle aggregation, such as the diffusion-limited aggregates, having a fractal dimension of $D_f\sim1.75$. Figure 8 shows an example of $C(t)$ obtained from a gold colloid aggregate having a basic particle diameter of 75 Å, and which is known to have a broad aggregate size distribution.[27] The stretched exponential analysis of such a curve is indeed possible with an exponent, $\beta=0.85$ which is still not low enough to explain the dynamic behavior of the microemulsion at $\phi\sim0.6$. A recent study by Martin[28] showed that a reaction-limited aggregate, which exhibits a power-law-

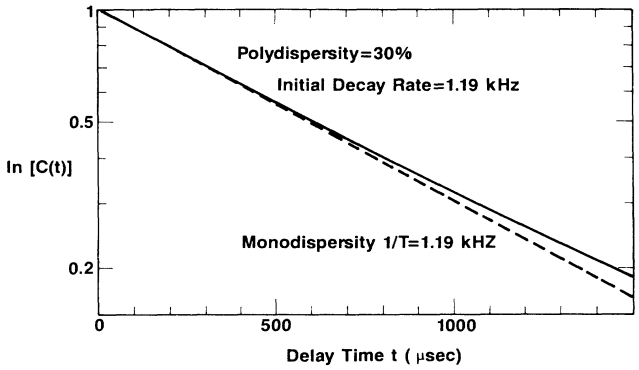

FIG. 6. Computer-simulated curves illustrating the effect of polydispersity on time behavior of the density correlation function for a system of Brownian particles. The dashed line corresponds to a noninteracting monodisperse system of particles of radius $R=65$ Å and the solid line a Schultz distributed polydisperse system of mean radius $\bar{R}=65$ Å and polydispersity index $p=0.3$. It is to be noted that the effect of polydispersity appears to produce slightly longer time tail in the density correlation function.

like size distribution, can stretch the density correlation function with a β value of 0.67. However, it has been known[5] that the polydispersity of the system studied is not powerlaw like. There, it can be safely concluded that $\beta=0.67$ is not due to polydispersity in our case.

Since the nonexponential behavior seems to be the dominant feature of the decay of the time-dependent density correlation function, our strategy of analyzing $C(t)$ to extract useful physical quantities could be as follows: we consider a multiple relaxation mechanism of some kind which leads to the nonexponential behavior. We therefore assert

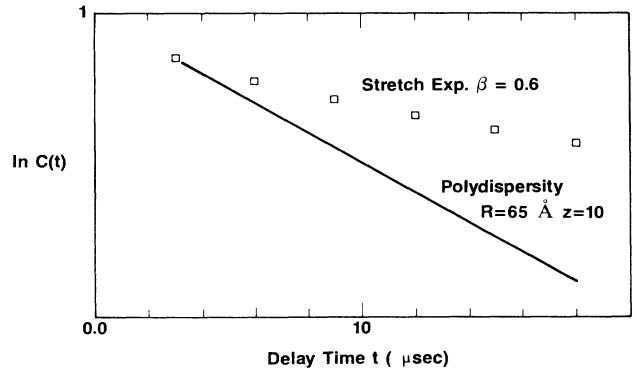

FIG. 7. Computer-simulated curves illustrating the qualitative difference between the density correlation functions for a polydisperse system of Brownian particles and a dense, interacting system of particles having the stretched exponential relaxation. This figure clearly shows that polydispersity alone cannot produce stretched exponential decay.

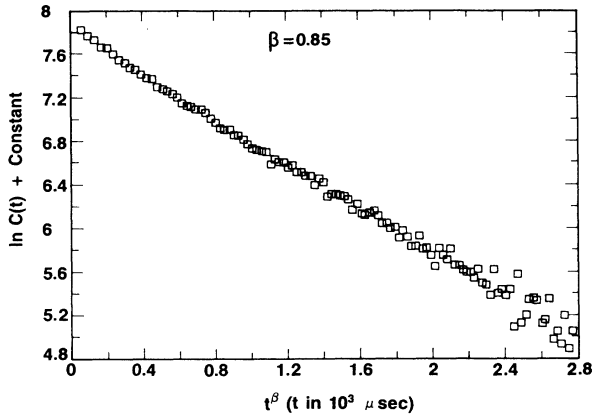

FIG. 8. This figure shows the logarithm of a correlation function obtained from a broad cluster distribution of diffusion-limited aggregates (DLA) of gold colloids with a fractal dimension of $D_f=2.0$. The mean aggregate size is roughly 5000 Å and the measured size distribution is a flat function over several decades of size with a cutoff around 1 μm. The correlation function can be analyzed with cumulant (K_i) expansion with $K_2/K_1\approx 0.3$. If we represent the correlation function by the Kohlraush-Williams-Watts function, the stretch exponent β would be around 0.85 (equivalent to an extremely polydisperse system), which is definitely outside the range of $0.5<\beta<0.7$ commonly observed near the glass-transition point.

$$C(t)=\int_0^\infty d\lambda\, f(\lambda)e^{-\lambda t}=\exp[-(t/\tau)^\beta]\ , \tag{6}$$

where $f(\lambda)$ is distribution function of the relaxation rate λ. The second equality in Eq. (6) cannot strictly be true at all time because according to the principle of the statistical mechanics, $C(t)$ has to decay exponentially at

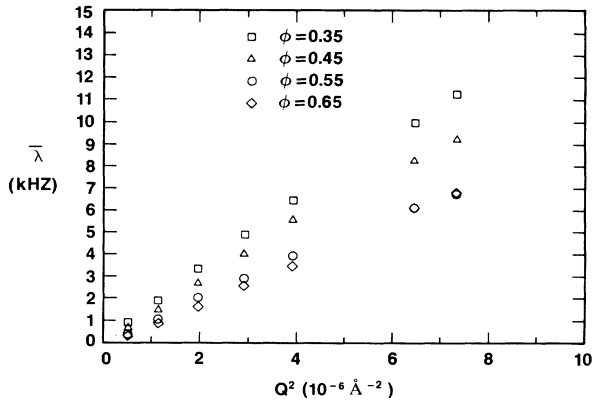

FIG. 9. Average relaxation rate $\bar{\lambda}$ of the density correlation function vs ϕ at different scattering angles for temperature equal to 22.6°C. Squares correspond to a 60° scattering angle, triangles to a 90° scattering angle, and diamonds to a 130° scattering angle. $\bar{\lambda}$ is extracted from the first cummulant of the density correlation function at short time. Interesting feature of these curves is that a minimum appears between $\phi=0.6$ and 0.65, which we define as ϕ_c, depending on the Q values in the scattering.

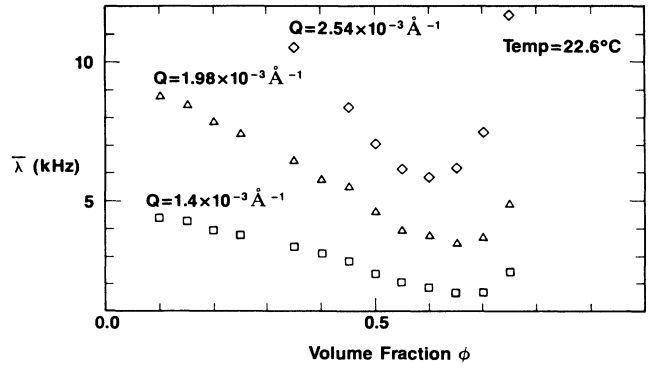

FIG. 10. The same plot as Fig. 9 for temperature equal to 17.9 °C and a scattering angle equal to 90° ($Q=1.98\times10^{-3}$ Å^{-1}). Note that no minimum appears in the vicinity of $\phi=0.6$, signifying a significant structural difference of microemulsions at $\phi=0.6$ between two temperatures, 22.6 °C and 17.9 °C.

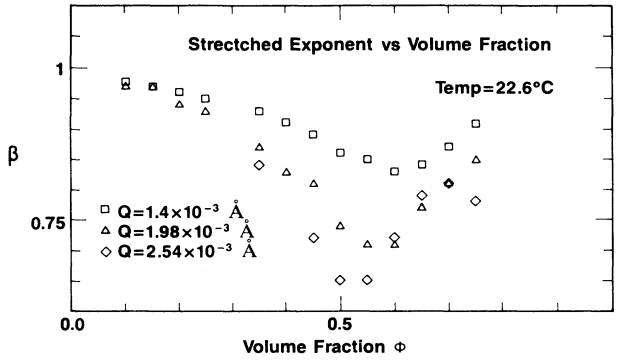

FIG. 12. The stretched exponent β as a function of ϕ at three Q values. Squares corresponds to $Q=1.4\times10^{-3}$ Å^{-1}, triangles to $Q=1.98\times10^{-3}$ Å^{-1}, and diamonds to $Q=2.54\times10^{-3}$ Å^{-1}. For these three scattering angles, a minimum β appear at $\phi=0.6$, 0.58, and 0.52, respectively.

both short times and long times. From Eq. (6) it follows that

$$\left.\frac{dC(t)}{dt}\right|_{t=0} = \int_0^\infty d\lambda\,\lambda f(\lambda)=\bar{\lambda}\ , \tag{7}$$

which equals the first cumulant, and the area A,

$$A=\int_0^\infty dt\,C(t)=\int_0^\infty d\lambda\,(1/\lambda)f(\lambda)$$
$$=\langle 1/\lambda\rangle=(1/\beta)\Gamma(1/\beta)\tau\ . \tag{8}$$

If, for example, we assume that $f(\lambda)$ has a bimodal distribution with a band of fast modes centering around λ_f and a band of slow modes around λ_s, then $\bar{\lambda}$ would be dominated by λ_f and $\langle 1/\lambda\rangle$ or equivalently $1/\beta\Gamma(1/\beta)T$ would be dominated by λ_s. It is thus obvious that the three most significant experimental quantities to be extracted are $\bar{\lambda}$, β, and τ. We first present the $\bar{\lambda}$ extracted from the first cumulant of $C(t)$ as a function of ϕ for various Q values at a temperature of 22.6 °C in Fig. 9. Figure 10 gives a similar plot for the case where the temperature is 17.9 °C at $Q=1.98\times10^{-3}$ Å^{-1}. It is noted that $\bar{\lambda}$ generally decreases as ϕ increases and shows a minimum between 0.6 and 0.65 at a temperature of 22.6 °C but exhibits no minimum for a temperature of 17.9 °C. Figure 11 shows that the average decay rate accurately follows Q^2 dependence. Moreover, the effective collective diffusion constant extracted from slopes of these curves shows a gradual decrease as ϕ increases.

Turning next to the results of stretched exponential fittings of $C(t)$, Fig. 12 shows dependence of the stretched exponent β as a function of volume fraction for three Q values at a temperature of 22.6°C. Figure 13 gives the same plot for $Q=1.98\times10^{-3}$ Å^{-1} at a temper-

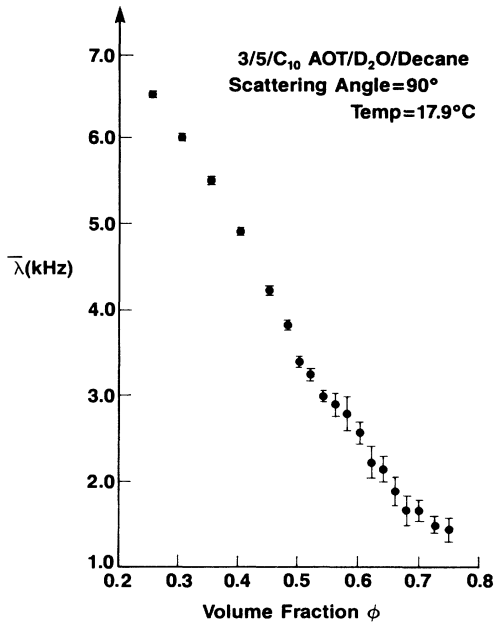

FIG. 11. Q^2 dependence of the average relaxation rates as a function of volume fractions ϕ. This figure shows that the effective collective diffusion constant decreases as ϕ increases.

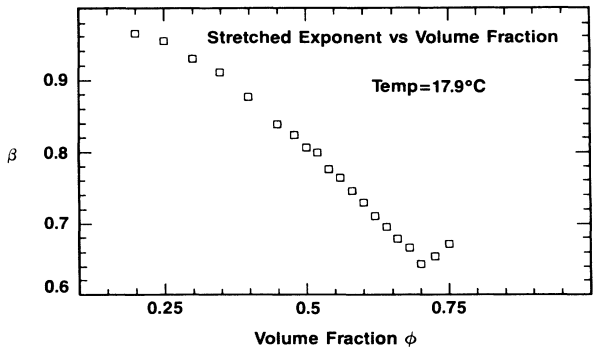

FIG. 13. Same plot as Fig. 12 for temperature equal to 17.9 °C. The minimum β occurs at $\phi=0.70$.

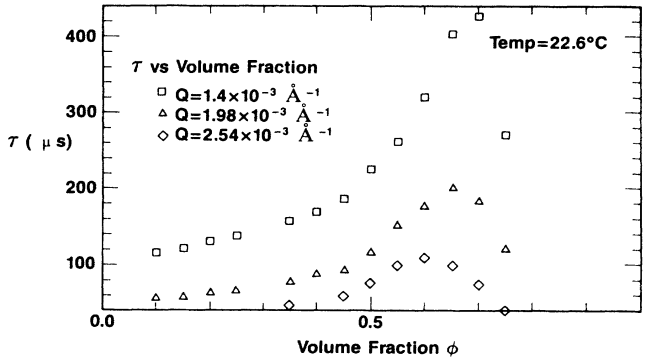

FIG. 14. Relaxation time τ vs ϕ plot for the high-temperature case at the three Q values. The relaxation time appears to reach maximum at $\phi=0.7$ for $Q=1.4\times10^{-3}$ Å^{-1}, 0.65 for $Q=1.98\times10^{-3}$ Å^{-1}, and 0.6 for $Q=2.54\times10^{-3}$ Å^{-1}.

ature of 17.9 °C. The extracted relaxation time τ is plotted as a function of ϕ for the three Q values at a temperature of 22.6 °C in Fig. 14. The same kind of plot is repeated in Fig. 15(a) for the temperature of 17.9 °C. Figure 15(b) gives the alternative plot of $\ln\tau$ versus $1/(\phi_c-\phi)$ for the same data shown in Fig. 15(a). A substantial difference has been noted between Figs. 14 and 15(a). For the high-temperature case (temperature of 22.6 °C), τ shows an apparent maximum at volume fraction between 0.6 and 0.7 but for the low-temperature case, τ shows a monotonic increase towards $\phi=0.75$.

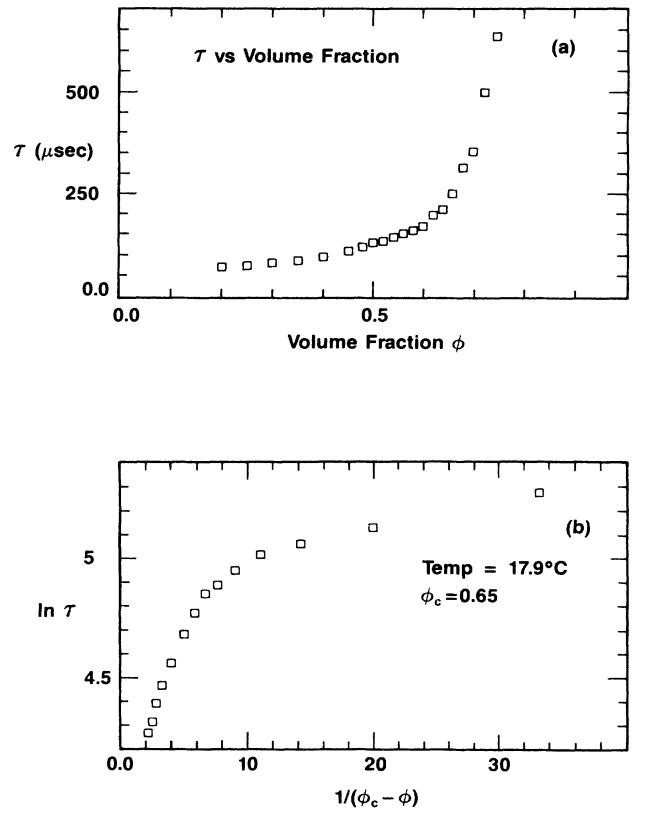

FIG. 15. The relaxation time τ vs ϕ plot for (a) the low-temperature case and (b) the Vogel-Fulcher plot assuming $\phi_c=0.65$. It is readily seen that as volume fraction approaches ϕ_c the Vogel-Fulcher plot exhibits linear behavior which is indicative of a glasslike transition.

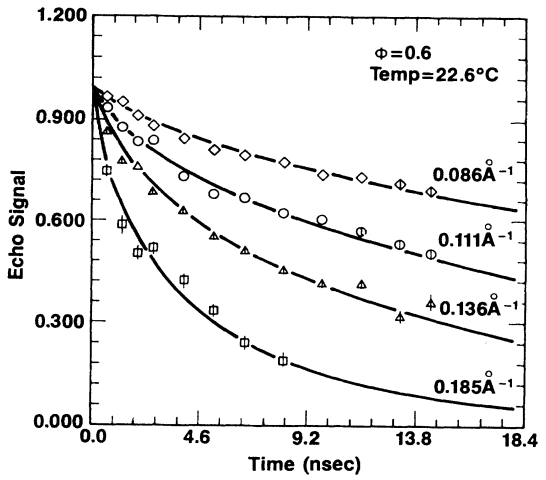

FIG. 16. The normalized intermediate scattering function $I(Q,t)$ obtained from neutron-spin-echo measurement for a AOT/D_2O/decane microemulsion with $w=40.61$ at $\phi=0.6$. The solid lines are the stretch-exponential fits to the measured value at different Q ranging from 0.086 to 0.185 Å^{-1}. The fits were made with β set equal to 0.67 but with various values of τ.

C. Neutron-spin-echo spectroscopy

Neutron-spin-echo spectroscopy[20] measures the normalized intermediate scattering funtion $I(Q,t)/S(Q)$ which is essentially the same as the normalized photon correlation functions, $C(t)$.[29] There is, however, a major difference in time scale of the measurement. While photon correlation function measures $C(t)$ at a time scale of milliseconds, the neutron-spin-echo spectroscopy measures at a time scale of nanoseconds. This is because the Q range of the two techniques differs by a factor of 10^3

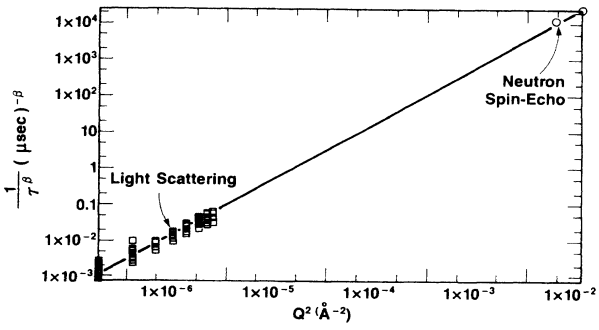

FIG. 17. $(1/\tau^{\beta})$ vs Q^2 plot for all data taken in QELS measurements and NSE experiments. Within the statistical spread of the data it fits a straight line going through the origin, over nearly six decades of the Q^2 range.

and the relaxation rates for c.m. diffusion scale like Q^2. We have measured a sample with $\phi=0.6$ at a temperature of 22.6 °C. Figure 16 shows the results of these measurements at four Q values, 0.086, 0.111, 0.136, and 0.185 Å^{-1}. The points are experimental data and the solid lines are the stretched exponential fits with $\beta=0.67$ and variable τ. Figure 17 summarizes all the photon correlation data and the neutron-spin-echo data in one graph. We plot the scaled relaxation time $\tau^{-\beta}$ for all volume fractions as a function of Q^2 in a log-log scale. The solid line is the straight line going through the data points having a slope equal to 2.

IV. DISCUSSIONS

It is clear from the experimental evidence presented in Figs. 2–17 that the properties of microemulsions around volume fraction $\phi_c=0.65$ exhibit anomalous behavior. In this discussion we shall review a set of specific data which lead us to conjecture that in the vicinity of $\phi=\phi_c$, due to dense packing of the microemulsion droplets, we can observe a glasslike transition in the dynamical behavior of the microemulsions.

We shall first look at the behavior of the viscosity as a function of volume fraction. According to mode-mode coupling theories of Leutheusser[10] and Bengtzelius, Goetz, and Sjolander,[11] the divergence of viscosity, or equivalently the vanishing of the self-diffusion constant, near the glass transition point can be described by a power-law-type divergence given by the following equation:

$$\eta=\eta_s(1-\phi/\phi_c)^{-\alpha} \tag{9}$$

for $\phi<\phi_c$ with $\alpha=1.8$. Angell has surveyed the applicability of this equation to a variety of glass-forming liquids [in this case ϕ is replaced by temperature in Eq. (9)] and concluded that α lies in the range of 1.5 to 2.5.[30] In Fig. 2(b) we present our viscosity data for a temperature of 22.6 °C in a plot of $(\eta_s/\eta)^{1/\alpha}$ versus ϕ/ϕ_c, $\phi_c=0.65$, for $\alpha=1.8$ and 2.5. The theoretical expression, Eq. (9), would correspond to a straight line connecting unity in the ordinate to unity in the abscissa. We see that the scaled data follow this relation approximately, especially, for $\alpha=2.5$. This is a first evidence that there might be a dynamic glass transition at $\phi_c=0.65$ as predicted by the mode-mode-coupling theories of density fluctuation. The mode-mode-coupling theories deal with a cage effect due to packing of spheres in a dense liquid which leads to vanishing of the self-diffusion coefficient. The evidence of dense packing of spheres for high volume fractions is well verified by the effective structure factors extracted from SANS data shown in Fig. 3. We attempted to fit the $S(Q)$ shown in Fig. 3 with Percus-Yevick theory of the structure factor for a hard-sphere system but without success.

The more convincing evidence of the glasslike transition, however, is supplied by the data from time-dependent correlation function measurements. Generally speaking, in a high-density liquid the density fluctuation can relax by two dominant mechanisms: (a) the high-frequency vibrational-type relaxation, and (b) a low-frequency diffusive-type relaxation. Due to the cage effect the low-frequency diffusional relaxation should be arrested at the glass-transition point, and the density correlation function should develop a DC component at the transition.[10,11,31] This trend is seen for the case of $\phi=0.68$ at a temperature of 17.9 °C in Fig. 4(b). It should be remarked here that microemulsion droplets are soft particles and presumably deformable at some slow rate. So, strictly speaking, a complete structural arrest can never take place by the cage effect alone. Here, we would not expect the density correlation function to develop a true DC component at any volume fraction. And it is then more meaningful to talk about the nonexponential decay of the correlation function as a function of volume fraction. Figures 5(a) and 5(b) illustrate very well that the time dependence of the correlation function can be accurately described by the KWW form for delay time from 100 to 1200 μs. Figures 6–8 also argue against the possibilities of the stretched exponential decay arising from polydispersity or aggregation of droplets. The average decay rate $\bar{\lambda}$ is shown to strictly obey Q^2 scaling in Fig. 11. It is thus dominated by a diffusive-type mode. It is, however, interesting to observe the $\bar{\lambda}$ decreases to variable minimum values $\phi_{\max}$ depending on the Q value as shown in Fig. 9. Due to the polydispersity of the droplets ($p=0.22$) the effective packing fraction for which the glass transition may occur should be higher than the volume fraction ϕ_c predicted for monodisperse hard spheres ($\phi_c=0.52$).[11] This is because as far as the cage effect is concerned only the volume fraction of larger spheres is relevant. The Q dependence of $\phi_{\min}$ which we attempted to identify as ϕ_c may be due to the polydispersity effect as well. It is puzzling, however, that $\bar{\lambda}$ do not show a minimum for the lower temperature sample (see Fig. 10). The β values shown in Figs. 12 and 13 seem to show both Q and temperature dependence. From Fig. 12 we observe the lowest β value, equal to 0.65, at a temperature of 22.6 °C and at largest Q value, 2.54×10^{-3} Å^{-1} (130° scattering angle). The minimum β value for $Q=1.4\times10^{-3}$ Å^{-1} case shifts up to 0.825. At the moment we do not have a theory for this effect. If we define ϕ_c by the volume fraction at which β reaches minimum as Q tends to zero, then ϕ_c could be obtained by extrapolating the minima in Fig. 12 to $Q=0$, which gives $\phi_c=0.68$. This is the reason we take $\phi_c=0.65$ in the analysis of our viscosity data in Fig. 2(b). From the result of Fig. 13 we would say that ϕ_c at a temperature of 17.9 °C is around 0.75. The maximum shown by the relaxation time τ given in Fig. 14 show the same trend of having a maximum at ϕ_c. Our data for τ for the case where the temperature is 17.9 °C are more complete and show that τ diverges at $\phi_c=0.75$ [see Fig. 15(a)]. We can therefore attempt to understand this divergent behavior at $\phi_c=0.75$. The plot shown in Fig. 15(b) indicates that near ϕ_c a relation such as

$$\tau=\tau_0\exp[K/(\phi_c-\phi)] \tag{10}$$

is valid. We may be able to identify this relaxation as Vogel-Fulcher law of relaxation time[32].

Lastly, Figs. 16 and 17 combine to show that the

stretched exponential behavior is valid in the entire Q range from 0.0014 Å^{-1} to 0.185 Å^{-1}. This includes the Q range for the structure factor from the hydrodynamic regime all the way up to the second diffraction peak regime.

V. CONCLUSION

The central theme of this paper is to show experimentally that the nonexponential decay of the time-dependent density correlation function in a dense microemulsion does not arise from polydispersity of the particle size, from an aggregation phonomena, (e.g., static percolation), but rather from dynamic correlations between spherical droplets packed in a dense liquidlike structure. This type of microemulsion system is thus an ideal model system for testing the current mode-mode coupling theories of dense liquids, and their prediction, of the glasslike transition.[10–16,33] Specifically, we have used shear viscosity measurement, small-angle neutron scattering, photon correlation spectroscopy, and neutron-spin-echo spectroscopy to study the transport coefficient, the static structure factor, and the dynamic structure factor in the whole range of volume fractions where the glasslike transition occurs. We showed that (a) the shear viscosity diverges at ϕ_c in a power-law behavior with $\alpha=2.5$, (b) the static structure factor near ϕ_c resembles that of densely packed spheres, (c) the average decay rate $\bar{\lambda}$ of the time-dependent density correlation function shows a minimum near $\phi=\phi_c$, (d) the time-dependent density correlation function follows, to an excellent approximation, the KWW form, $\exp[-(t/\tau)^{\beta}]$, at long time over at least two decades of decay time, (e) the stretched exponent β, starting from unity at $\phi=0.1$, gradually decreases to a lower value depending on the Q value of the scattering experiment. The lowest value observed is $\beta=0.64$ at $\phi=0.70$ for $\tau=17.9\,^{\circ}\text{C}$ and $Q=1.98\times10^{-3}$ Å^{-1}, (f) the relaxation time τ, on the other hand, increases toward ϕ_c and shows a divergent behavior similar to the Vogel-Fulcher law, and finally, the stretched exponential behavior is also observed by NSE at high-Q value beyond the first diffraction peak of the structure factor. Thus, to a good approximation the stretched exponential behavior of the time-dependent density correlation function is independent of Q in the entire relevant range from $Q=1.4\times10^{-3}$ Å^{-1} to 0.185 Å^{-1} and the relaxation time τ scales like $Q^{-2/\beta}$.

ACKNOWLEDGMENTS

The authors are grateful to Bela Farago and Dieter Richter for providing the neutron-spin-echo measurements. We also acknowledge the Brookhaven National Laboratory for granting beam time on H9B of the high flux beam reactor, and technical assistance from Dieter Schneider. This research is supported by a NSF grant administered by Center for Materials Science & Engineering of MIT and by Exxon Research & Engineering Company.

[1](a) S. H. Chen, T. L. Lin, and J. S. Huang, in *Physics of Complex and Supermolecular Fluids,* edited by S. A. Safran and N. A. Clark (Wiley, New York, 1987), pp. 285–313; (b) M. Kotlarchyk, S. H. Chen, J. S. Huang, and M. W. Kim, Phys. Rev. A **29**, 2054 (1984).
[2]M. Zulauf and H. F. Eicke, J. Phys. Chem. **83**, 480 (1979).
[3]C. Cabos and P. Delord, J. Appl. Crystallogr. **12**, 502 (1979).
[4]M. Kotlarchyk, S. H. Chen, and J. S. Huang, J. Phys. Chem. **86**, 3273 (1982).
[5]M. Kotlarchyk, S. H. Chen, J. S. Huang, and M. W. Kim, Phys. Rev. A **29**, 2054 (1984).
[6]M. Kotlarchyk, S. H. Chen, J. S. Huang, and M. W. Kim, Phys. Rev. Lett. **9**, 941 (1984).
[7]J. S. Huang and M. W. Kim, Phys. Rev. Lett. **47**, 1452 (1981).
[8]M. Kotlarchyk, S. H. Chen, and J. S. Huang, Phys. Rev. A **28**, 508 (1983).
[9]Per. Ekwall, L. Mandell, and K. Fontell, J. Coll. Int. Sci. **33**, 215 (1970).
[10]E. Leutheusser, Phys. Rev. A **29**, 2765 (1984).
[11]U. Bentzelius, W. Goetze, and A. Sjolander, J. Phys. Chem. **17**, 5915 (1984).
[12]W. Gotze and L. Sjogren, Z. Phys. B **65**, 415 (1987).
[13]T. Kirkpatrick, Phys. Rev. A **31**, 939 (1985).
[14]U. Bentzelius, Phys. Rev. A **33**, 3433 (1986).
[15]S. P. Das and G. F. Mazenko, Phys. Rev. A **34**, 2265 (1986).
[16]G. H. Fredrickson, Ann. Rev. Phys. Chem. **39**, 149 (1988).
[17]Eric Y. Sheu, S. H. Chen, and J. S. Huang, J. Phys. Chem. **91**, 3306 (1987).
[18]S. H. Chen and T. L. Lin, *Methods of Experimental Physics—Neutron Scattering,* edited by K. Sköld and L. D. Price (Academic, Orlando, 1987), Vol. II, Chap. 16, pp. 489–543.
[19]J. S. Huang, B. Farago, and D. Richter (unpublished).
[20]For review of the neutron-spin-echo technique, see, for instance F. Mezei, in *Neutron Spin-Echo,* Vol. 128 of *Lecture Notes in Physics,* edited by F. Mezei (Springer-Verlag, Berlin, 1979).
[21]M. Kotlarchyk and S. H. Chen, J. Chem. Phys. **79**, 2461 (1983).
[22]S. H. Chen and Eric Y. Sheu, Makromol. Chem. Macromol. Symp. **15**, 275 (1988).
[23]P. Van Beurten and A. Vrij, J. Chem. Phys. **74**, 2744 (1981).
[24]S. H. Chen, Eric Y. Sheu, J. Kalus, and H. Hoffmann, J. Appl. Crystallogr. **21**, 751 (1988).
[25]C. F. Wu, Eric Y. Sheu, D. Bendedouch, and S. H. Chen, Kinam **8A**, 37 (1987).
[26]M. W. Kim and J. S. Huang, Phys. Rev. A **34**, 719 (1986).
[27]D. A. Weitz, J. S. Huang, M. Y. Lin, and J. C. Sung, Phys. Rev. Lett. **54**, 1416 (1985).
[28]J. Martin, Phys. Rev. A **36**, 3415 (1987).
[29]J. B. Hayter, *Scattering Techniques Applied to Supramolecular and Nonequilibrium Systems,* edited by S. H. Chen, B. Chu, and R. Nossal (Plenum, New York, 1981), p. 49.
[30]C. A. Angell, Phys. Chem. Solids (to be published).
[31]P. N. Pusey and W. van Megen, Phys. Rev. Lett. **59**, 2083 (1987).
[32]M. I. Klinger, Phys. Rep. **165**, 275 (1988).
[33]U. Bengtzelius and A. Sjolander, Ann. N.Y. Acad. Sci. **484**, 229 (1986).